

Quantum simulation of many-body spin interactions with ultracold polar molecules

Hendrik Weimer*

Institut für Theoretische Physik, Leibniz Universität Hannover, Appelstr. 2, 30167 Hannover, Germany

(Dated: September 10, 2018)

We present an architecture for the quantum simulation of many-body spin interactions based on ultracold polar molecules trapped in optical lattices. Our approach employs digital quantum simulation, i.e., the dynamics of the simulated system is reproduced by the quantum simulator in a stroboscopic pattern, and allows to simulate both coherent and dissipative dynamics. We discuss the realization of Kitaev's toric code Hamiltonian, a paradigmatic model involving four-body interactions, and we analyze the requirements for an experimental implementation.

PACS numbers: 03.67.Ac, 34.20.Gj, 05.30.Pr

I. INTRODUCTION

The realization of quantum simulators – devices which can replicate the dynamics of other quantum systems [1, 2] – is currently one of the most exciting topics in the field of ultracold quantum gases [3]. This is particularly relevant in areas where classical simulation methods have proven to be inadequate due to the exponential growing Hilbert space dimension, such as in frustrated quantum magnets, where the system sizes that can be studied using exact diagonalization methods are typically limited to less than 50 spins [4, 5].

Ultracold polar molecules are particularly promising candidates for the quantum simulation of spin models due to their long coherence times and strong electric dipole interactions at distances compatible with optical addressing. In the past, several theoretical proposals have been made for the realization of quantum magnetism in these systems [6–14]. However, these proposals are challenging to extend to higher order many-body interactions as these terms arise within a perturbation series and thus become exponentially weaker the more particles participate in the interaction [6, 7]. On the other hand, such spin models with many-body interactions have recently received great attention in the context of Kitaev's toric code Hamiltonian [15], which has interesting topological properties, and for the generation of cluster states, which are relevant for measurement-based quantum computing [16].

In this article, we describe an architecture for an efficient non-perturbative simulation of many-body spin interactions. Our approach is related to a recent quantum simulation proposal based on strongly interacting Rydberg atoms [17, 18]; however, due to the inherent limitations to Rydberg excitations due to their fast radiative decay, an implementation with ultracold polar molecules within their electronic ground state manifold might offer some beneficial aspects. Our approach to quantum simulation will be a digital one, i.e., the dynamics of the simulated system arises stroboscopically at discrete time

intervals [2]. In particular, the effective dynamics will be created by applying sequences of microwave pulses coupling rotational excitations of the polar molecules, realizing sequences of single-body and two-body quantum logic gates. We first describe the setup composed of ultracold polar molecules trapped in optical lattices, followed by a discussion on the implementation of a single many-body interaction. Besides coherent time evolution, the quantum simulator is also capable to incorporate dissipative dynamics, including efficient preparation of the ground state. We will then generalize these concepts to the full lattice system and discuss the sources and consequences of residual imperfections. Finally, we describe the experimental requirements to implement our quantum simulation architecture.

II. SETUP OF THE SYSTEM

We consider a two-dimensional system of ultracold polar molecules in their rovibrational ground state [19, 20]

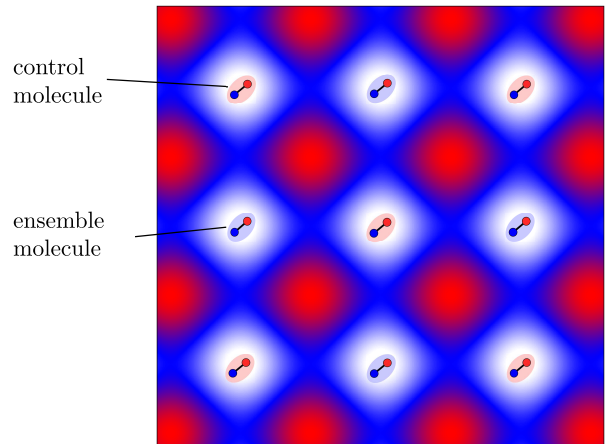


FIG. 1: Proposed experimental setup. Polar molecules are arranged in the intensity minima of a two-dimensional optical lattice with one molecule per lattice site. Molecules on neighboring lattice sites take different roles as control or ensemble molecules.

*Electronic address: hweimer@itp.uni-hannover.de

and loaded into an optical lattice [21], see Fig. 1. We focus on the case where the lattice potential is deep enough to suppress any tunneling between different sites. Furthermore, we assume the molecules to be initially prepared in a well-defined hyperfine state [22]. Here, we are also interested in a setup where a single *control molecule* is surrounded by four *ensemble molecules*, in a way that the former can be manipulated independently without affecting the other ones. Such a controllability is most readily achieved if the molecules can be addressed individually using optical fields [23]. Note that the distinction between control and ensemble molecules is a purely logical one, i.e., both types can be realized using a single molecular species.

The relevant level structure of the molecules is shown in Fig. 2, where we focus on the lowest four rotationally excited states. We consider the driving of rotational transitions by microwave fields. By combining linearly and circularly polarized microwaves together with the electric quadrupole interaction coupling the nuclear spin to the rotation (δ) [24], it is possible to selectively drive transitions between hyperfine states [22].

Additionally, we are interested in the situation where a strong linearly polarized microwave field Ω_0 is resonant with the transition between the states $|J = 2, m_I\rangle$ and $|J = 3, m_I\rangle$. The quantization axis is defined by the polarization, so the dynamics will be constrained to states with vanishing projection of the angular momentum on the quantization axis, i.e., $J_z = 0$. In the dressed frame of this driving described by the Hamiltonian

$$H_0 = \Omega_0 |J = 2, m_I\rangle \langle J = 3, m_I| + \text{h.c.}, \quad (1)$$

the state $|-\rangle = (|J = 2\rangle - |J = 3\rangle)/\sqrt{2}$ will pick up an effective permanent dipole moment of $d_e = 3d/\sqrt{70}$, where d is the bare electric dipole moment of the molecule [11]. Additionally, we consider a weak microwave driving Ω of the two-photon transition between the state $|0\rangle$ and the dressed state $|-\rangle$.

Finally, the position of the $|-\rangle$ manifold can be shifted relative to the $|J = 0\rangle$ manifold using optical fields resulting in a differential ac Stark shift [25], which can shift the molecules out of resonance of the microwave field Ω . By confining the optical potentials to individual lattice sites, single molecule addressing on a lengthscale of 500 nm can be realized [23]. Further improvements might be achieved using sub-wavelength addressing techniques using strong field gradients [26] or electromagnetically induced transparency [27].

Essentially, the setup presented here allows to selectively create rotational excitations, depending of the position of the molecule and its hyperfine state. Consequently, the dynamics is effectively constrained to three states: two nuclear states corresponding to the $|J = 0\rangle$ manifold (named $|0\rangle$ and $|1\rangle$ hereafter), and one state in the $|-\rangle$ manifold ($|2\rangle$). The benefit of this setup based on microwave dressing compared to ones involving static electric fields lies in the strong suppression of dipolar flip-flop terms coupling different J states, thus eliminating a

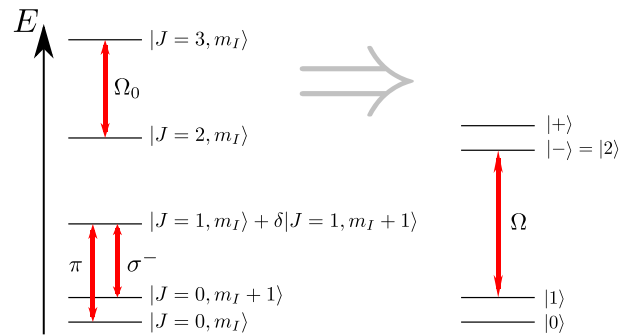


FIG. 2: Relevant part of the internal level structure. Depending on the polarization of microwave fields (π, σ^\pm), hyperfine-preserving or hyperfine changing transitions can be driven. A strong microwave field Ω_0 couples the $J = 2$ manifold to the $J = 3$ manifold, resulting in dressed states that can be accessed by an additional two-photon microwave driving Ω . For the purpose of the quantum simulator, only the states $|0\rangle$, $|1\rangle$, and $|2\rangle$ are important.

potential error source for the quantum simulator.

III. SIMULATION OF THE TORIC CODE

The specific model we want to outline a quantum simulator for is Kitaev’s toric code [15]. It serves as paradigmatic model of a large class of so-called *stabilizer Hamiltonians* [28, 29], whose ground states can be found by local minimization of the energy. The toric code Hamiltonian is given by

$$H = -E_0 \left(\sum_p A_p + \sum_v B_v \right), \quad (2)$$

with the “plaquette” operators $A_p = \prod_{i \in p} \sigma_x^{(i)}$ and the “vertex” operators $B_v = \prod_{i \in v} \sigma_z^{(i)}$ containing Pauli operators representing four-body spin interactions, see Fig. 3. On a torus, the ground state of the toric code is four-fold degenerate and corresponds to the +1 eigenvalues of all mutually commuting operators A_p and B_v and exhibits topological order. Plaquettes or vertices with a -1 eigenvalue are quasiparticles called *magnetic charges* or *electric charges*, respectively, and always occur in pairs with a string operator connecting them [15]. Due to the non-commutativity of σ_x and σ_z , moving a quasiparticle of one type around a second one of the other type will result in a minus sign applied to the quantum state; hence, the quasiparticles of the toric code are abelian anyons.

These exotic properties have led to many proposed realizations within ultracold quantum gases or condensed matter systems [6, 17, 18, 30–33], but despite experimental success in small systems [34, 35], a large-scale many-body implementation revealing the topological properties is still lacking [36]. In the following, we will discuss the implementation of the toric code within our quantum

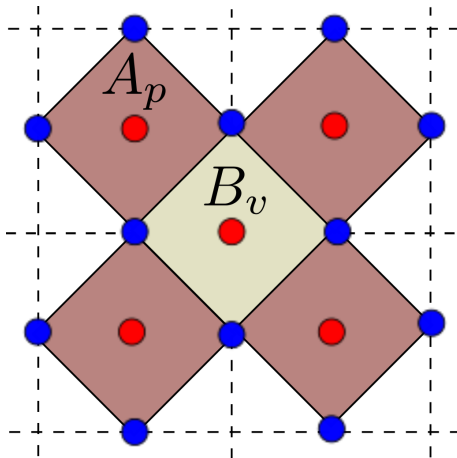


FIG. 3: Two-dimensional lattice setup for the toric code involving control (red) and ensemble molecules (blue). The ensemble molecules taking part in plaquette operators A_p and vertex operators B_v are colored accordingly.

simulator architecture. As all terms of the Hamiltonian are mutually commuting, the dynamics of the toric code can be constructed by sequential implementation of the plaquette terms and vertex terms, i.e.,

$$U = \exp(-iHt) = \prod_p \exp(iE_0 A_p t/\hbar) \prod_v \exp(iE_0 B_v t/\hbar). \quad (3)$$

The form of the plaquette interactions A_p and the vertex interactions B_v is identical up to a global rotation interchanging σ_x and σ_z ; hence, we focus first on the implementation of a single B_v term, with all remaining terms of the Hamiltonian to be realized in an analogous way.

A. Single plaquette interaction

As a crucial step, we now make use of the control molecules to mediate the vertex interaction. During this process, we require the implementation of single qubit rotation between the logical states $|0\rangle$ and $|1\rangle$. Such single qubit gates between nuclear spin states have already been experimentally realized based on the electric quadrupole moment of the nucleus [22]. Furthermore, our architecture will involve a two-qubit controlled phase gate between two molecules, which we will present in the following.

1. Controlled phase gate

The two logical states $|0\rangle$ and $|1\rangle$ do not exhibit any dipole-dipole interactions, hence, it is necessary to first transfer the population from the $|1\rangle$ state to the $|2\rangle$ state by a two-photon microwave pulse. Doing this simultaneously in the control molecule and a single ensemble

molecule requires the microwave driving Ω to be much stronger than the dipole-dipole interaction,

$$V_{dd} = \frac{1}{4\pi\epsilon_0} \frac{d_e^2}{a^3}, \quad (4)$$

where a is the separation between the control and the ensemble molecule. After the pulse, the molecules experience the dipole-dipole interaction for the time $t_\pi = \pi\hbar/V_{dd}$, following a second microwave pulse transferring the population back to the rovibrational ground state. Then, up to local rotations which can be canceled by appropriate additional driving fields, the system has realized a conditional phase gate of the form

$$U_{CP}^{(e)} = |0\rangle\langle 0|^{(c)} \otimes 1^{(e)} + |1\rangle\langle 1|^{(c)} \sigma_z^{(e)}, \quad (5)$$

where c and e refer to the control and ensemble molecule, respectively.

2. Digital simulation procedure

We will now turn to the quantum simulation of the vertex term B_v in the toric code Hamiltonian (2). During a single timestep τ of our digital quantum simulator, a single vertex undergoes the time evolution $U = \exp(iE_0 B_v \tau)$. Such a dynamics is realized by a three-fold sequence, provided the control molecule is initially in $|0\rangle_c$ [17, 18]: (i) A sequence of quantum gates maps the eigenvalue ± 1 of the operator B_v acting on the ensemble molecules is mapped onto the states $|0\rangle$ and $|1\rangle$ of the control molecule, i.e., performing the operation

$$U_{\text{MAP}} = |0\rangle\langle 0|_c |B_v = 1\rangle\langle B_v = 1| + (|0\rangle\langle 1|_c + |1\rangle\langle 0|_c) |B_v = -1\rangle\langle B_v = -1|. \quad (6)$$

(ii) A single qubit rotation of the form $U_Z(\phi) = \exp(i\phi\sigma_z^{(c)})$ is applied to the control molecule. (iii) The mapping of step (i) is undone by the inverse gate sequence. The total gate sequence for the simulation of the time evolution reads

$$U = \exp(i\phi B_v) = U_{\pi/2}^{(c)} \prod_e U_{CP}^{(e)} U_{-\pi/2}^{(c)} U_Z(\phi) U_{\pi/2}^{(c)} \prod_e U_{CP}^{(e)} U_{-\pi/2}^{(c)}, \quad (7)$$

where $U_{\pi/2}^{(c)} = \exp(i\sigma_y \pi/4)$ is a $\pi/2$ rotation of the control molecule. This sequence involves a series of four controlled-phase gates U_{CP} acting on the control molecule and each ensemble molecule sequentially, which effectively represents a multi-qubit gate, where the control molecule conditionally manipulates the ensemble molecules, sometimes denoted as a Controlled-Phase^N quantum gate. This sequential operation offers maximum speed of the gate sequence as all operations can be carried out resonantly. On the other hand, conceptually slightly simpler but slower gate sequences based on direct multi-qubit gates [37] also exist [17, 18].

The effective energy scale E_0 of the simulated Hamiltonian depends on the phase ϕ written onto the control molecule during each timestep τ , i.e., $E_0 = \hbar\phi/\tau$. While for the toric code involving only mutually commuting operators, ϕ can be arbitrarily large, models with non-commuting degrees of freedom mandate the introduction of a Trotter expansion of the form $\exp(-iH\tau) = \prod_i \exp(-iH_i\tau) + O(\tau^2)$, requiring $\phi \ll 1$ to reproduce the desired dynamics with high accuracy.

3. Dissipative state preparation

As already mentioned, the ground state of the toric code Hamiltonian (2) can be found by locally minimizing the energy of the stabilizer operators A_p and B_v . Therefore, it is possible to engineer the dynamics such that energy is constantly removed from the system and the ground state arises as the final state of the dynamics [17, 18, 38, 39]. As a crucial element, the dissipation of energy requires the presence of an incoherent process in the dynamics; here, we are interested in the situation where the control molecule can be incoherently pumped from the state $|1\rangle$ to the state $|0\rangle$. However, such a dissipative step is not as straightforward to realize as with atoms since the radiative decay of molecules to many vibrational states makes optical pumping very challenging. Essentially, possible experimental realizations of the desired dissipative dynamics can be generalized into three distinct classes: (i) Direct laser cooling of molecules [40, 41], giving rise to sufficiently high optical pumping efficiencies. (ii) Microwave driving of the $|1\rangle$ state to a rotationally excited state, which is strongly coupled to the $|0\rangle$ state via a lossy microwave stripline resonator [42, 43]. (iii) Employing hyperfine-preserving STIRAP processes to dissociate molecules back into atoms, followed by optical pumping of the atoms and reversing the STIRAP process.

For the implementation of dissipative state preparation, we employ the gate sequence

$$U = U_{CNOT,i} U_{\pi/2}^{(c)} U_{CP} U_{\pi/2}^{(c)}, \quad (8)$$

where $U_{CNOT,i}$ is a controlled-NOT gate with the control molecule as a control qubit and the i th ensemble molecule acting as a target qubit. This two-body gate can be easily constructed from the controlled phase gate U_{CP} using additional single qubit rotations. The action of the gate sequence U can be understood by looking at the states $|\pm, \lambda\rangle$ having the property $\langle B_v \rangle = \pm 1$ (here, λ encodes the information about the state that is independent of B_v). The chosen gate sequence will yield

$$U|0\rangle_c |\pm, \lambda\rangle_e = \frac{1 \pm 1}{2} |0\rangle_c |+1, \lambda\rangle_e + \frac{1 \mp 1}{2} |1\rangle_c |+1, \lambda\rangle_e. \quad (9)$$

Note that both summands contain the state $|+1, \lambda\rangle_e$ for the ensemble molecules, as the final controlled-NOT gate transforms the state $|1\rangle_c |-1, \lambda\rangle$ into $|1\rangle_c |+1, \lambda\rangle$ while

leaving the $|0\rangle_c |+1, \lambda\rangle$ state untouched. Performing the dissipative step $|1\rangle_c \rightarrow |0\rangle_c$ results in the state $|+1, \lambda\rangle$ for the ensemble molecules, independent of λ . In general, the dynamics created by U and subsequent dissipation can be described in terms of a discrete time quantum master equation in Lindblad form,

$$\rho(t + \tau) = c\rho(t)c^\dagger - \frac{1}{2} \{c^\dagger c, \rho(t)\}, \quad (10)$$

with the quantum jump operator $c = i\sigma_x^{(i)}(1 - B_v)/2$. This jump operator consists of the projector $(1 - B_v)/2$ forming an *interrogation part* that checks whether the system is in a $+1$ eigenstate of B_v and a *pump part* $\sigma_x^{(i)}$, which flips a single spin and thus turns any state with $B_v = -1$ into a state with $B_v = +1$. From the toric code Hamiltonian it is obvious that the jump operator changing $B_v = -1$ to $+1$ will lower the energy of the system and thus constitute a cooling effect. Indeed, by performing this cooling operation many times on all vertices and plaquettes, we can prepare the ground state of the toric code [17, 18].

B. Full lattice model

As shown above, it is possible to construct a quantum simulation of the toric code for both coherent and dissipative dynamics by iterating over all plaquettes and vertices in the full lattice system. For maximum performance, it is desirable to exploit the largest degree of parallelism, while keeping errors at a minimum. While it is possible to address many molecules in parallel at the same time, one has to be aware of a few limitations. First, one has to make sure that any parallel implementation

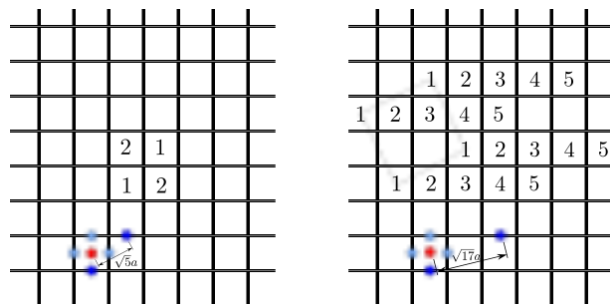


FIG. 4: Sublattice schemes for the toric code. Numbers from 1 to z indicate which plaquettes are being addressed simultaneously. As exemplified for a single control atom (red) performing a two-qubit gate with the ensemble molecule located immediately below (dark blue), there is crosstalk with an ensemble molecule associated to a different plaquette. Inactive ensemble molecules surrounding the control molecule that are shown in light blue for reference. For a simple $z = 2$ partitioning scheme, the dominant contribution to the crosstalk occurs at a distance of $\sqrt{5}a$, while for a $z = 5$ scheme with a knight's move unit cell, the distance is increased to $\sqrt{17}a$.

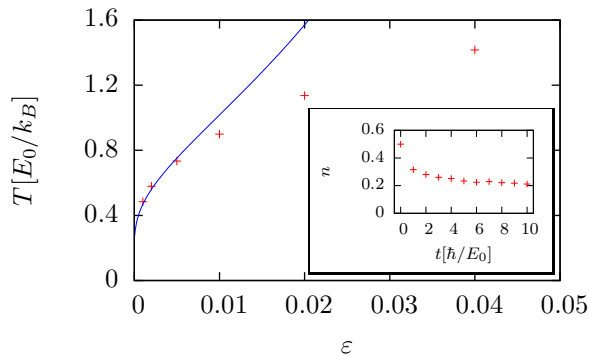


FIG. 5: Dependence of the residual temperature T on the two qubit gate error probability ϵ . Numerical simulation for a system of 16 ensemble molecules averaged over 1000 realizations are shown as crosses, while the solid line is derived within linear response theory. The inset shows the relaxation dynamics for $\epsilon = 0.01$.

of plaquette and vertex operators does not try to address the same molecule twice during a single operation. This is naturally enforced by operating plaquette and vertex operations sequentially and partitioning the system into two different sublattices ($z = 2$), see Fig. 4. Second, the long-range tail of the dipole-dipole interaction will introduce errors due to crosstalk between molecules on different plaquettes or vertices. This effect can be reduced by increasing the unit cell of the sublattice. Already by using a $z = 5$ sublattice arranged in a knight’s move pattern, the crosstalk can be reduced to a percent level perturbation.

C. Imperfections

In any realistic experimental situation, there will be other sources of imperfections besides crosstalk between distant molecules due to the long range dipolar interaction, such as phase noise of the laser fields used for optical addressing of individual molecules. Here, the dominant source of error will be related to the two qubit controlled phase gates. Effectively, such errors can be described in terms of a random phase flip σ_z acting on one of the qubits with probability ϵ . These gate errors will lead to additional noise terms in the quantum master equation [17], and for the toric code will result in a finite anyon density n , which can be cast as an effective temperature T , according to

$$T \approx -\frac{2E_0}{k_B \log n}. \quad (11)$$

Applying linear response theory to the quantum master equation (10), we can obtain an asymptotic expres-

sion for the anyon density $n = 4c\epsilon$, with the numerical constant c depending on the details of the error model. In the case of phase errors, we find $c = 7/2$. As shown in Fig. 5, this behavior is reproduced by numerical simulations in the limit of small gate errors. Remarkably, already for gate errors on the order of $\epsilon \approx 0.01$, the stationary state reaches a low temperature regime characterized by $k_B T/E_0 < 1$, where topological order can be detected within finite-size systems [44, 45].

IV. EXPERIMENTAL REQUIREMENTS

To be specific, we focus on an implementation using NaK molecules [46], which combine chemical stability [47] with a relatively large electric dipole moment of $d = 2.7D$. Single qubit operations can be carried out with a speed of ~ 20 kHz [22] and hence will be much faster than the two-qubit conditional phase gates. For the latter, we obtain a gate speed of $t_\pi^{-1} \approx 2$ kHz for an $a = 532$ nm optical lattice, according to Eq. (4). The overall timescale E_0 for the simulation of the toric code will be lower due to the subsequent implementation of plaquette and vertex operators and the need for partitioning the system into several sublattices. Here, for the aforementioned $z = 5$ partition scheme, we obtain $E_0 = h \times 40$ Hz, which is compatible with typical timescales in experiments with ultracold polar molecules. For comparison, although the Rydberg quantum simulator can reach energy scales up to three orders of magnitudes larger [17], the polar molecule quantum simulator can achieve similar results for coherence times on the order of $t_c \sim 100$ ms, corresponding to a two qubit gate error of $\epsilon \approx t_\pi/t_c = 0.005$.

V. CONCLUSION AND OUTLOOK

In summary, we have demonstrated the feasibility of a quantum simulator for many-body spin interactions using ultracold polar molecules trapped in optical lattices. The proposed architecture includes both coherent and dissipative dynamics and is quite robust against experimental imperfections, as we have exemplified for the toric code Hamiltonian. At the same time, the setup naturally allows for extensions to even larger classes of strongly correlated spin models, paving the way towards the realization of a universal quantum simulator based on ultracold polar molecules.

Acknowledgments

We acknowledge fruitful discussions with S. Ospelkaus.

-
- [1] R. P. Feynman, *Int. J. Theor. Phys.* **21**, 467 (1982).
- [2] S. Lloyd, *Science* **273**, 1073 (1996).
- [3] I. Bloch, J. Dalibard, and S. Nascimbène, *Nature Phys.* **8**, 267 (2012).
- [4] H. Nakano and T. Sakai, *J. Phys. Soc. Jpn.* **80**, 053704 (2011).
- [5] A. M. Läuchli, J. Sudan, and E. S. Sørensen, *Phys. Rev. B* **83**, 212401 (2011).
- [6] A. Micheli, G. K. Brennen, and P. Zoller, *Nature Phys.* **2**, 341 (2006).
- [7] H. P. Büchler, A. Micheli, and P. Zoller, *Nature Phys.* **3**, 726 (2007).
- [8] A. V. Gorshkov, S. R. Manmana, G. Chen, J. Ye, E. Demler, M. D. Lukin, and A. M. Rey, *Phys. Rev. Lett.* **107**, 115301 (2011).
- [9] A. V. Gorshkov, S. R. Manmana, G. Chen, E. Demler, M. D. Lukin, and A. M. Rey, *Phys. Rev. A* **84**, 033619 (2011).
- [10] D. Peter, S. Müller, S. Wessel, and H. P. Büchler, *Phys. Rev. Lett.* **109**, 025303 (2012).
- [11] M. Limeshko, R. V. Krems, and H. Weimer, *Phys. Rev. Lett.* **109**, 035301 (2012).
- [12] N. Y. Yao, C. R. Laumann, A. V. Gorshkov, S. D. Bennett, E. Demler, P. Zoller, and M. D. Lukin, *Phys. Rev. Lett.* **109**, 266804 (2012).
- [13] N. Y. Yao, A. V. Gorshkov, C. R. Laumann, A. M. Läuchli, J. Ye, and M. D. Lukin, *arXiv:1212.4839* (2012).
- [14] A. V. Gorshkov, K. R. A. Hazzard, and A. M. Rey, *arXiv:1301.5636* (2013).
- [15] A. Y. Kitaev, *Ann. Phys.* **303**, 2 (2003).
- [16] R. Raussendorf, S. Bravyi, and J. Harrington, *Phys. Rev. A* **71**, 062313 (2005).
- [17] H. Weimer, M. Müller, I. Lesanovsky, P. Zoller, and H. P. Büchler, *Nature Phys.* **6**, 382 (2010).
- [18] H. Weimer, M. Müller, H. P. Büchler, and I. Lesanovsky, *Quant. Inf. Proc.* **10**, 885 (2011).
- [19] K.-K. Ni, S. Ospelkaus, M. H. G. de Miranda, A. Pe'er, B. Neyenhuis, J. J. Zirbel, S. Kotochigova, P. S. Julienne, D. S. Jin, and J. Ye, *Science* **322**, 231 (2008).
- [20] J. Deiglmayr, A. Grochola, M. Repp, K. Mörtlbauer, C. Glück, J. Lange, O. Dulieu, R. Wester, and M. Weidemüller, *Phys. Rev. Lett.* **101**, 133004 (2008).
- [21] M. H. G. de Miranda, A. Chotia, B. Neyenhuis, D. Wang, G. Quemener, S. Ospelkaus, J. L. Bohn, J. Ye, and D. S. Jin, *Nature Phys.* **7**, 502 (2011).
- [22] S. Ospelkaus, K.-K. Ni, G. Quémener, B. Neyenhuis, D. Wang, M. H. G. de Miranda, J. L. Bohn, J. Ye, and D. S. Jin, *Phys. Rev. Lett.* **104**, 030402 (2010).
- [23] C. Weitenberg, M. Endres, J. F. Sherson, M. Cheneau, P. Schauß, T. Fukuhara, I. Bloch, and S. Kuhr, *Nature* **471**, 319 (2011).
- [24] J. Brown and A. Carrington, *Rotational Spectroscopy of Diatomic Molecules* (Cambridge University Press, Cambridge, 2003).
- [25] S. Kotochigova and D. DeMille, *Phys. Rev. A* **82**, 063421 (2010).
- [26] K. D. Stokes, C. Schnurr, J. R. Gardner, M. Marable, G. R. Welch, and J. E. Thomas, *Phys. Rev. Lett.* **67**, 1997 (1991).
- [27] A. V. Gorshkov, L. Jiang, M. Greiner, P. Zoller, and M. D. Lukin, *Phys. Rev. Lett.* **100**, 093005 (2008).
- [28] D. Gottesman, *Phys. Rev. A* **54**, 1862 (1996).
- [29] H. Bombin and M. A. Martin-Delgado, *Phys. Rev. Lett.* **97**, 180501 (2006).
- [30] L.-M. Duan, E. Demler, and M. D. Lukin, *Phys. Rev. Lett.* **91**, 090402 (2003).
- [31] G. Jackeli and G. Khaliullin, *Phys. Rev. Lett.* **102**, 017205 (2009).
- [32] A. E. B. Nielsen and K. Mølmer, *Phys. Rev. A* **82**, 052326 (2010).
- [33] A. G. Fowler, M. Mariani, J. M. Martinis, and A. N. Cleland, *Phys. Rev. A* **86**, 032324 (2012).
- [34] C.-Y. Lu, W.-B. Gao, O. Gühne, X.-Q. Zhou, Z.-B. Chen, and J.-W. Pan, *Phys. Rev. Lett.* **102**, 030502 (2009).
- [35] J. T. Barreiro, M. Müller, P. Schindler, D. Nigg, T. Monz, M. Chwalla, M. Hennrich, C. F. Roos, P. Zoller, and R. Blatt, *Nature* **470**, 486 (2011).
- [36] N. Lang and H. P. Büchler, *Phys. Rev. A* **86**, 022336 (2012).
- [37] M. Müller, I. Lesanovsky, H. Weimer, H. P. Büchler, and P. Zoller, *Phys. Rev. Lett.* **102**, 170502 (2009).
- [38] M. Aguado, G. K. Brennen, F. Verstraete, and J. I. Cirac, *Phys. Rev. Lett.* **101**, 260501 (2008).
- [39] F. Verstraete, M. M. Wolf, and J. Ignacio Cirac, *Nature Phys.* **5**, 633 (2009).
- [40] E. S. Shuman, J. F. Barry, and D. DeMille, *Nature* **467**, 820 (2010).
- [41] I. Manai, R. Horchani, H. Lignier, P. Pillet, D. Comparat, A. Fioretti, and M. Allegrini, *Phys. Rev. Lett.* **109**, 183001 (2012).
- [42] A. André, D. DeMille, J. M. Doyle, M. D. Lukin, S. E. Maxwell, P. Rabl, R. J. Schoelkopf, and P. Zoller, *Nature Phys.* **2**, 636 (2006).
- [43] M. Wallquist, P. Rabl, M. D. Lukin, and P. Zoller, *New J. Phys.* **10**, 063005 (2008).
- [44] C. Castelnovo and C. Chamon, *Phys. Rev. B* **76**, 184442 (2007).
- [45] Z. Nussinov and G. Ortiz, *Phys. Rev. B* **77**, 064302 (2008).
- [46] C.-H. Wu, J. W. Park, P. Ahmadi, S. Will, and M. W. Zwierlein, *Phys. Rev. Lett.* **109**, 085301 (2012).
- [47] P. S. Żuchowski and J. M. Hutson, *Phys. Rev. A* **81**, 060703 (2010).